



# Plant Archives

Journal homepage: <http://www.plantarchives.org>  
 DOI Url : <https://doi.org/10.51470/PLANTARCHIVES.2023.v23.no1.001>

## STUDY OF MUNG BEAN ISOFLAVONES ASSOCIATED WITH ENHANCED ANTIOXIDANT ACTIVITY HAVING THERAPEUTIC IMPLICATIONS

Sujoy Kumar Sen<sup>1,2,3</sup>, Palash Mandal<sup>2</sup>, and Jnan Bikash Bhandari<sup>3\*</sup>

<sup>1</sup>Department of Botany, Siliguri College, Darjeeling, West Bengal, India-734 001, ORCID Id: 0000-0002-9828-5694

<sup>2</sup>Nanobiology and Phytotherapy Laboratory, Department of Botany, University of North Bengal, Darjeeling, West Bengal, India-734 013, ORCID Id: 0000-0003-0742-7931

<sup>3</sup>Pteridology and Palaeo Botany Laboratory, West Bengal, India-734 013, ORCID Id: 0000-0002-5573-4760

\*Corresponding Author: [jnanbikashbhandari@nbu.ac.in](mailto:jnanbikashbhandari@nbu.ac.in)

(Date of Receiving : 15-01-2023; Date of Acceptance : 20-03-2023)

### ABSTRACT

Isoflavonoids have a wide range of biological effects. The majority of them could be helpful, while some could be dangerous, depending on the circumstances. These are plant secondary metabolites that, through a variety of metabolic pathways, mediate numerous biological functions. They are structurally related to estrogen and progesterone and have estrogenic and antiestrogenic effects in various tissues. Legumes are rich in proestrogenic isoflavones such Biochanin A and Formononetin, which are the starting points for the methylation of genistein and daidzein. In the current study, the effects of solid matrix priming (SMP), which uses nano-chitosan to treat salt stress in mung bean sprouts, were assessed. The findings demonstrated that isoflavone concentration in mung bean sprouts considerably increased after SMP with nano-chitosan. The chosen isoflavones also underwent an in-silico drug trial and toxicity assessment.

**Keywords** : Drug study; in silico; isoflavones; mung bean; nano-chitosan; solid matrix priming.

### Introduction

The mung bean, a type of popular leguminous pulse crop, is mainly grown due to its high economic value and beneficial health advantages. As sprouts, daal, cakes, noodles, snacks, and more, it plays a significant role in the predominantly cereal-based diets of many Asian countries, including India. Legume-centric diets are associated with improvements in human health over the long term by reducing the risks of diabetes, cardiovascular disease, and a variety of malignancies (Lamartiniere *et al.*, 1998). Isoflavonoids are natural compounds that belong to plant secondary metabolites and mediate diverse biological functions through numerous pathways. Being structurally similar to estrogens, they exert estrogenic and antiestrogenic properties. They promote human health. Due to a variety of bioprotective actions, such as antioxidant, antimutagenic, anticarcinogenic, and antiproliferative activities, which are primarily evaluated in vitro, interest in the potential health advantages of isoflavonoids has developed (Yamagata & Yamori 2021; Birt *et al.*, 2001; Ryan-Borchers *et al.*, 2006). They have traditionally been thought of as dietary antioxidants that might prevent oxidative stress associated with the severe danger of damages from free radicals and other related oxygen and nitrogen-based oxidizing agents (Reiter *et al.*, 2008). They could defend the body against hormone-related cancers like breast, uterine, and prostate

cancer. They are also associated with a wide range of health-protective properties, such as immunomodulation, risk reduction of chronic diseases like cardiovascular disease, diabetes, cancer, osteoporosis, obesity, and relief of menopausal symptoms (Ryan-Borchers *et al.*, 2006; Mir *et al.*, 2022; Bezek *et al.*, 2008; Birt *et al.*, 2001). Notably, though some Epidemiologic studies investigating the function of isoflavonoids supports the preventive advantages of isoflavonoid supplementation as a natural alternative to oestrogen replacement medication, other studies were unable to show such benefits and thus showing conflicting results.

One of the many toxicological endpoints of chemical substances that is of great concern is carcinogenicity due to the negative effects it has on people's health. To stop the spread of drug-induced cancer, pharmaceutical companies must conduct numerous carcinogenicity studies prior to receiving marketing approval for their novel medications (Zhang *et al.*, 2017). However, in recent years, computer methods for predicting carcinogenicity based on chemical structural properties have supplanted animal model tests due to their time-consuming, expensive, unethical, and labor-intensive nature (Raies & Bajic, 2006).

Due to their structural resemblance to other known active chemicals, the compounds examined in this study may have pharmacological effects. To assess if a chemical can be employed as a medicinal agent, pharmacokinetics and

pharmacodynamics are frequently used. The pharmacokinetic phase is made up of the absorption, distribution, metabolism, and elimination (ADME) of the drug. It is commonly accepted that early pharmacological development should include screening for and altering ADME features (Wang and Skolnik, 2009). Analyzing ADME attributes quickly can save time and money. Skin sensitization is a crucial component of the intricate immune-mediated inflammatory skin reaction that occurs in allergic contact dermatitis disease and significantly affects the patient's quality of life and functional capacity. Pred-Skin, an accessible and reliable web tool, can be used in this situation to confirm early skin sensitization brought on by chemicals. The *in vivo* test of choice for assessing the possibility of cutaneous sensitization is the murine local lymph node assay (LLNA) (Basketter *et al.*, 2002).

The purpose of the current investigation is the quantitative study and standardization of major mung bean isoflavones through HR-LCMS of mung bean sprouts (treated, and untreated) grown under salinity stress conditions, and their *in silico* analysis associated with the therapeutic implications in humans along with their correlations with salt stress-related genes using the online resources, and web-tools are also chief ideas of the current work.

## Materials and Methods

### Collection and sterilization of mung bean seeds

The Pulse and Oilseed Research Station in Berhampur, West Bengal, India provided the mung bean [*Vigna radiata* (L.) R. Wilczek] cultivar (SAMRAT). The seeds were thoroughly washed with 70% ethanol. Then, the seeds were surface sterilized by a 4% sodium hypochlorite (NaOCl) solution for 10 min, followed by a thorough washing of the seeds several times with autoclaved double distilled water

### Preparation and characterization of nano-chitosan

In this study, the ionic gelation method was used to create nano-chitosan using chitosan and sodium tripolyphosphate (STPP) as a cross-linking agent (Rajeshwari *et al.*, 2016). Spectra of scanning electron microscopy (SEM), transmission electron microscopy (TEM), dynamic light scattering (DLS), Fourier transform infrared (FTIR), and X-ray diffraction (XRD) were used to characterize the nano-chitosan. SEM, TEM and XRD analysis of prepared nano-chitosan sample (powder) was conducted from SAIF IIT Bombay.

### Germination setup and sample preparation

Sterilized seeds were placed to separate, airtight zipper bags (10.5 cm 7.8 cm) containing 1g of Celite (used as a matrix) that was kept at a 10% moisture level by nano-chitosan for the purpose of seed priming. After 24 hours of priming, seeds were taken out of the matrix, dried, and stored overnight in the fridge. The seeds were stored for seven days under observation while they germinated in the seed germinator.

### Chromatograms derived from High-Resolution Liquid Chromatography-Mass Spectrometry (HR-LCMS)

Three isoflavone standards viz., Biochanin A (MW 284.26, Sigma – D2016-100 MG), Genistein (MW 270.24, Sigma G6649-5 MG), Formononetin (MW 268.26, Sigma 344215-5MG) were purchased and used for HR-LCMS.

Methanolic extracts (samples) of treated mung bean seedlings, along with the 3 isoflavone standards, were subjected to HR-LCMS. Identification of metabolites from an active subfraction of chloroform extract was carried out at the Sophisticated Analytical Instrument Facility (SAIF), IIT, Bombay, Powai, Mumbai-400076.

### Toxicity Evaluation

In the current study, to evaluate the toxicologic characteristics of the selected phytochemicals, including isoflavones, Pred-hERG (<http://lab-mol.farmacacia.ufg.br/predherg/>), and the CarcinoPred-EL (Carcinogenicity Prediction using Ensemble Learning methods) were employed (<http://ccsibp.lnu.edu.cn/toxicity/CarcinoPred-EL/>). The SMILES strings of the chemicals that are to be predicted by the user can be entered into the textbox. At one moment, up to 1000 molecules can be processed in CarcinoPred-EL. Further, to evaluate putative skin sensitizers freely available Pred-Skin web tool (<http://labmol.com.br/predskin/>) was used to perform rapid virtual screening of the chosen phytochemicals under study. Xenosite reactivity (<https://swami.wustl.edu/xenosite/p/reactivity>) was also carried out for screening the toxicity test of isoflavones and the metabolites under the current study. The three isoflavones under research reacted with DNA to determine which molecule might potentially create DNA adducts. This was done using the online tool Xenosite reactivity (Djoubou-Feunang *et al.*, 2019; Muegge *et al.*, 2001; Delannée *et al.*, 2019).

### The gene-set functional enrichment analysis and protein-protein interaction networks

The STRING data set version 11.5 (<https://string-db.org>) was used for the gene-set functional enrichment analysis and the protein-protein interaction networks. The acronym STRING stands for Search Tool for the Retrieval of Interacting Genes/Proteins. To calculate the topological gene score, STRING-generated interaction data was fed into Cytoscape (version 3.8.2; <https://cytoscape.org/>) software.

## Results and Discussion

### Characterization of nano-chitosan

The SEM image of nano-chitosan (Figure 1A) shows that it has a more or less uniform structure, which is quite different from chitosan. These results back up what Sivakami *et al.* (2013) found before. Figure 1B shows a TEM image of nano-chitosan, which shows that the nanoparticles are somewhat round in shape. DLS technique is employed to measure both how easily chitosan nanoparticles move in the light and how big they are in size (Dubin, 1967). Because of the uncertain Brownian motion of the chitosan nanoparticles in this dispersion, the intensity of the scattered light varies with time. The polydispersity index (PDI) of the chitosan nanoparticles was found to be 0.465, and an early correlation coefficient decay curve was made (Figure 1C). In terms of size distribution, the chitosan-TPP binary electrolyte system sometimes had TPP cross-linked nano-chitosan. It was found that the zeta potential of nanoparticles made from chitosan is +100 mV. (Figure 1D). Because the surface charge was increased, the performance was even more impressive. The spectra of chitosan and nano-FTIR chitosan are shown in (Figures 1E). The hydrogen-bonded O-H stretching vibration makes the solid and broad peak in the 3500-3300 range of the chitosan spectrum. In this area, the N-H stretching peaks of

type II amide and primary amines are the same (Yu *et al.*, 1999). The peak of the FTIR spectrum of nano-chitosan moves from 3438  $\text{cm}^{-1}$  to 3433.12  $\text{cm}^{-1}$  as the relative intensity goes up. This means that the peak is getting bigger. This shows how hydrogen bonds are getting better. Also, the peaks for the N-H bending vibration of the amide-II carbonyl stretch and the amine-I carbonyl stretch moved to 1600  $\text{cm}^{-1}$  and 1650  $\text{cm}^{-1}$ , respectively. Another P-O peak was found at 1629.83  $\text{cm}^{-1}$ . These results proved that there is a link between phosphoric and ammonium ions. Figure 1-F shows the XRD patterns and surface topography of nano-chitosan. X-ray diffraction patterns were used to look at the amorphous and crystalline structures of the material. The XRD data for nano-chitosan was collected using an X-ray diffractometer with an X-ray tube, a sample holder, and an X-ray detector, as well as CuK1 irradiance at 50 kV. The fact that nano-chitosan was crystalline was shown by the XRD pattern.

### Isoflavone content and derivation of the mung bean Isoflavonoids (KEGG pathway)

Isoflavones are a separate class of secondary plant metabolites that are produced by the phenylpropanoid pathway. They are primarily generated by members of the Papilionaceae family (Wang and Murphy 1994). The chromatograms of three primary isoflavones detected in mung bean sprouts Biochanin-A, Formononetin, and Genistein as determined by quantitative LC-MS analysis are shown in Figure 2. It is possible to describe the production of mung bean isoflavonoids using the KEGG pathway of the flavonoid biosynthesis route. According to the KEGG pathway, Naringenin is converted into Genistein by route of

2-hydroxy-2, 3-dihydrogenistein ( $\text{C}_{15}\text{H}_{12}\text{O}_6$ ). The chemical reaction that results in Genistein is conducted by the enzyme 2-hydroxyisoflavanone dehydratase [EC: 4.2.1.105]. The reaction's substrate is 2, 7, 4'-trihydroxyisoflavanone. Genistein is subsequently converted directly into Biochanin-A ( $\text{C}_{16}\text{H}_{12}\text{O}_5$ ) by the enzyme isoflavone 4'-O-methyltransferase [EC: 2.1.1.212 2.1.1.46] (Figure 3). Genistein with S-Adenosyl-L-Methionine leads to Biochanin with S-Adenosyl-L-homocysteine-A. Genistein is additionally converted into the compounds Genistein 7-O-beta-D-glucoside ( $\text{C}_{21}\text{H}_{20}\text{O}_{10}$ ), Prunetin ( $\text{C}_{16}\text{H}_{12}\text{O}_5$ ), or 2'-hydroxygenistein ( $\text{C}_{15}\text{H}_{10}\text{O}_6$ ) by the enzymes isoflavone 7-O glucosyltransferase (EC: 2.4.1.170) and isoflavone-7-O methyltransferase (EC: 2. 1.1.150). Daidzein, Formononetin, and Glycitein are all precursors to the flavanone Liquiritigenin (7,4'-dihydroxyflavanone), whereas Genistein and Biochanin-A are precursors to Naringenin (5,7,4'-dihydroxyflavanone). Liquiritigenin, or 4', 7-Dihydroxyflavanone ( $\text{C}_{15}\text{H}_{12}\text{O}_4$ ), is converted into 2, 7, 4'-Trihydroxyisoflavanone ( $\text{C}_{15}\text{H}_{12}\text{O}_5$ ) by the enzyme 2-hydroxyisoflavanone dehydratase (EC: 4.2.1.105), which in turn transforms Daidzein ( $\text{C}_{15}\text{H}_{10}\text{O}_4$ ) into Formononetin ( $\text{C}_{16}\text{H}_{12}\text{O}_4$ ) by the activity of isoflavone 4'. An interesting fact about ononin is that it is an isoflavone glycoside. It is the 7-O-D-glucopyranoside of Formononetin, which is itself a 4'-O-methoxy derivative of the parent isoflavones Daidzein.

In mung bean seedlings cultivated under salt stress, Formononetin, Genistein, and Biochanin-A were found to be significant isoflavones in the chitosan-primed, nano-chitosan primed, and untreated control, respectively (Table 1).

**Table 1 :** Identified isoflavone content in mung bean seedlings under salinity stress after different treatments.

Sl. No.	Treatment	Salinity stress (dS/m)	Identified Isoflavone	Peak Area	Peak Height	Calculated Avg conc. (ppm)
1	Nano-chitosan Priming	4	Genistein	22046.13	2510.02	6.20
2	Unprimed Control	4	Biochanin-A	6037762.09	599392.69	2.39
3	Chitosan Priming	4	Formononetin	31511479.69	2539862.25	9.98

### In Silico study: ADME, Bioactivity prediction, and Toxicity analysis

The ADME analysis of the three chosen isoflavones was successful, and toxicity screening was then carried out to assess the efficacy and level of indemnity of the chosen isoflavones. Table 2 displays ADMET, the druggability of the selected isoflavones, as well as their water and lipophilicity solubility properties.

The plotted BOILED-Egg prediction model and RADAR diagrams for Biochanin A, Formononetin, and Genistein are shown in Figures 4 (A) and 4 (B-D), respectively. The pink area in the RADAR diagrams corresponded to the most advantageous zone for each of the bioavailability parameters. Using the swissADME web tool, the accuracy of the ADME results and toxicity prediction were verified. To evaluate the three chosen phytochemicals' drug-likeness, toxicology analysis and ADME criteria were applied.

**Table 2 :** ADME and the druggability of the selected isoflavones.

ADMET Properties	Biochanin A	Formononetin	Genistein
Formula	$\text{C}_{16}\text{H}_{12}\text{O}_5$	$\text{C}_{16}\text{H}_{12}\text{O}_4$	$\text{C}_{15}\text{H}_{10}\text{O}_5$
Molecular weight	284.26 g/mol	268.26 g/mol	270.24 g/mol
Num. heavy atoms	21	20	20
Num. arom. heavy atoms	16	16	16
Fraction Csp3	0.06	0.06	0.00
Num. rotatable bonds	2	2	1
Num. H-bond acceptors	5	4	5
Num. H-bond donors	2	1	3
Molar Refractivity	78.46	76.43	73.99
Topological Polar Surface Area (TPSA)	79.90 $\text{\AA}^2$	59.67 $\text{\AA}^2$	90.90 $\text{\AA}^2$
Log $P_{\text{o/w}}$ (iLOGP)	2.55	2.49	1.91
Log $P_{\text{o/w}}$ (XLOGP <sub>3</sub> )	2.99	2.80	2.67

Log $P_{o/w}$ (WLOGP)	2.88	3.17	2.58
Log $P_{o/w}$ (MLOGP)	0.77	1.33	0.52
Gastrointestinal (GI) absorption	High	High	High
Blood-brain-barrier (BBB) permeant	No	Yes	No
Poly-glycoprotein (P-gp) substrate	No	No	No
Lipinski	0	0	0
Ghose	0	0	0
Veber	0	0	0
Egan	0	0	0
Muegge	0	0	0
Bioavailability Score	0.55	0.55	0.55
PAINS	0 alert	0 alert	0 alert
Brenk	0 alert	0 alert	0 alert
Leadlikeness	Yes	Yes	Yes
Synthetic accessibility	2.89	2.81	2.87

The findings indicate that all three of the chosen phytochemicals had high gastrointestinal (GI) absorption rates. Similar results were obtained with Biochanin-A and Genistein, both of which had low toxicity and no BBB permeability. Formononetin, however, showed good blood-brain barrier (BBB) penetration. The BBB can be compared to armour that protects the brain by creating a biochemical and physical barrier (consisting of enzymatic activities and active efflux). Despite its importance, passive diffusion is the main mechanism by which medicines enter the brain from the bloodstream (Di *et al.*, 2012). The white region represents the physicochemical space of the compounds displaying the maximum likelihood of absorption by the gastrointestinal system, and the yolk represents the maximum probability to permeate to the brain in the BOILED-Egg predictive model for the three isoflavones. It should be emphasised, though, that the yolk and white portions are not exclusive. It was noted that Biochanin-A and Genistein, respectively, demonstrated the highest and lowest Molar Refractivity, iLOGP, and XLOGP3.

Additionally, Genistein displayed the lowest WLOGP and MLOGP values, whereas Formononetin displayed the highest values. According to Genistein and Biochanin-A, respectively, the highest and lowest topological Polar Surface Area (TPSA) was demonstrated.

For the chosen compounds, other rules of drug-likeness were also checked, including Lipinski's rule of five, Ghose's rule, Veber's rule, Egan's rule, and Muegge's rule (Daina *et al.*, 2017; Lipinski *et al.*, 1997; Ghose *et al.*, 1999; Egan *et al.*, 2000; Veber *et al.*, 2002). None of the three phytochemicals violated any of Lipinski's five rules, which include the Ghose, Veber, Egan, and Muegge filters.

Through PASS, pharmacological actions for Biochanin A, Formononetin, and Genistein were anticipated (Table 3). These isoflavones are particularly important therapeutically as antimutagenic, cardioprotective, and antineoplastic drugs, according to the PASS prediction.

**Table 3 :** Pharmacological activities are predicted through PASS for Biochanin A, Formononetin, and Genistein.

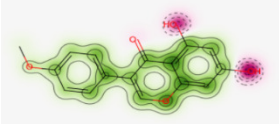
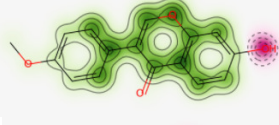
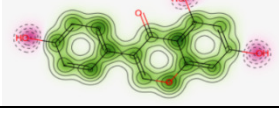
Compound	Main predicted properties by PASS online	Pa*	Pi*
Biochanin A	Antimutagenic	0,869	0,003
	Antihypercholesterolemic	0,783	0,005
	Vasoprotector	0,776	0,006
	Cardioprotectant	0,731	0,004
	Anticarcinogenic	0,727	0,008
	Antineoplastic	0,735	0,020
	Antiseborrheic	0,803	0,018
	DOPA decarboxylase inhibitor	0,725	0,001
	Breast cancer-resistant protein inhibitor	0,869	0,001
	MAO-A inhibitor	0,754	0,002
	MAO-B inhibitor	0,704	0,002
HMOX1 expression enhancer	0,723	0,006	
Formononetin	Antimutagenic	0,831	0,003
	Antiseborrheic	0,807	0,018
	Apoptosis agonist	0,731	0,012
Genistein	Antimutagenic	0,874	0,003
	Antiseborrheic	0,832	0,013
	Vasoprotector	0,822	0,004
	Antioxidant	0,765	0,004
	Cardioprotectant	0,742	0,004
	Antineoplastic	0,750	0,018
Monophenol monooxygenase inhibitor	0,920	0,002	

Figure 5(A) displays the probability maps for the PRED SKIN characteristics of Biochanin A, Formononetin, and Genistein. Particularly noteworthy are the Pred-hERG Analysis results in Table 4, which present the probability maps for Biochanin A, Formononetin, and Genistein.

Table 5 lists the CarcinoPred-EL characteristics of Genistein, Formononetin, and Biochanin A. According to predictions made using the xenosite reactivity 2.0 resource tool (Djoumbou-Feunang *et al.*, 2019; Delannée *et al.*, 2019),

Figures 5 (B-D) shows the DNA reactivity of the potential metabolites of phase I metabolism of Biochanin A, Formononetin, and Genistein, respectively. Glutathione is employed as a marker of drug toxicity, and this method can also predict a molecule's reaction with cyanide, GSH, and proteins. The region of reactivity is shown by a circle in the molecule's structure, and these predictions are represented by a colour shade with a score of 0 to 1.

**Table 4 :** Comparative Pred-hERG Analysis of Biochanin A, Formononetin, and Genistein.

Isoflavones	Prediction/potency	Confidence	Applicability domain	Probability map
Biochanin A	Non-cardiotoxic	70%	No (Value = 0.25 and Limit = 0.26)	
Formononetin	Non-cardiotoxic	70%	Yes (Value = 0.25 and Limit = 0.26)	
Genistein	Non-cardiotoxic	70%	No (Value = 0.19 and Limit = 0.26)	

**Table 5 :** CARCINO PRED EL of Biochanin A, Formononetin, and Genistein (\*NC= non-carcinogen; CDK, CDKExt, CDKGraph, KR, KRC, MACCS & Pubchem are the seven fingerprints).

Isoflavones	Method	CDK	CDKExt	CDKGraph	KR	KRC	MACCS	Pubchem	Avg	Class
Biochanin -A	RF	0.45	0.41	0.26	0.47	0.57	0.42	0.37	0.42	NC
	SVM	0.39	0.39	0.24	0.50	0.45	0.25	0.32	0.36	NC
	XGBoost	0.07	0.19	0.47	0.45	0.62	0.63	0.76	0.46	NC
Formononetin	RF	0.46	0.43	0.29	0.47	0.56	0.51	0.37	0.44	NC
	SVM	0.38	0.44	0.28	0.47	0.49	0.37	0.32	0.40	NC
	XGBoost	0.07	0.19	0.47	0.50	0.60	0.63	0.76	0.45	NC
Genistein	RF	0.44	0.41	0.34	0.41	0.42	0.29	0.38	0.38	NC
	SVM	0.39	0.37	0.30	0.48	0.39	0.19	0.32	0.35	NC
	XGBoost	0.07	0.19	0.47	0.45	0.53	0.63	0.76	0.44	NC

### String and Cytoscape analysis

The results of the String and Cytoscape experiments to ascertain how the chosen isoflavones interact with the salt stress genes are shown in Figures 6A and 6B, respectively. Some genes, such as SOS1, SOS2, SOS3, CBL1, CBL10, NHX1, AKT1, and VPS34, are identified as having an impact in how the seedlings respond to salinity stress (pathway ID GO: 0009651). Also, the genes SOS3, CBL3, and NHX1 control how much potassium is in the plant body (pathway ID GO: 0055075). Ion transporters, like the Na<sup>+</sup>/H<sup>+</sup> antiporter SALT OVERLY SENSITIVE 1 (SOS1) and the K<sup>+</sup> rectifier ARABIDOPSIS K<sup>+</sup> TRANSPORTER 1 (AKT1), keep the K<sup>+</sup>/Na<sup>+</sup> ratio in the cytoplasm at the right level. This is an important part of being able to handle salt (Chen *et al.*, 2005; Feng *et al.*, 2015). These secondary transporters receive their energy from the concentration gradients made by transmembrane proton pumps like plasma membrane H<sup>+</sup>-ATPase, vacuolar H<sup>+</sup>-ATPase (V-ATPase), and vacuolar H<sup>+</sup>-translocating inorganic pyrophosphatase (V-PPase) (Chen *et al.*, 2010; Yuan *et al.*, 2016). It is essential that the plasma membrane H<sup>+</sup>-ATPase is a critical necessity that can be affected by saline stress, cold stress, heavy metal stress, and

stress from active transport of the stressor across the plasma membrane (Martz *et al.*, 2006; Shi *et al.*, 2008; Janicka-Russak *et al.*, 2012). In *Arabidopsis thaliana*, the genes ACC1, CAC1, and BCCP2 control fatty acid biosynthesis (KEGG pathway ID 00061), fatty acid metabolism (KEGG pathway ID 01212), and pyruvate metabolism (KEGG pathway ID 00620). BCCP2, CAC1, KIN11, ACC1, ACC2, and VPS34 genes of *Arabidopsis thaliana* are also associated with the procedure of cellular lipid metabolism (pathway ID: 0044255). Astonishingly, acetyl-CoA also plays a role in acetylation of histones. This gives peroxisomal FA oxidation influence over epigenetic modifications in the nucleus, which may affect a number of cellular mechanisms (Wang *et al.*, 2019).

So, salinity, which is one of the most important and harsh abiotic stress factors, hurts the output of mung bean seedlings all over the world. Under salt stress, plants store too many sodium (Na<sup>+</sup>) and chloride (Cl<sup>-</sup>) ions. This leads to both physiological and biochemical problems like ionic inequity, changes in water homeostasis, and the production of more ROS. It also starts phytotoxic responses like lipid peroxidation, which stops enzymes from working, and

protein degradation, which breaks down proteins (Farooq *et al.*, 2018; Cao *et al.*, 2011). Plants produce osmolytes like proline, carbohydrates, and other substances to combat this adverse oxidative stress, which decreases the cellular water potential and helps water uptake by keeping the right water gradient. By turning on the genes that control the metabolic shifting of key isoflavones, enzymatic antioxidants like SOD, CAT, APX, and GPX and non-enzymatic metabolites like flavonoids, proline, and ascorbic acid worked together to reduce the negative effects of ROS and increase tolerance to salinity stress. The salinity tolerance framework is interconnected to the generation of reactive oxygen species (ROS), signal transduction, detoxifying pathways, ion homeostasis, and the appearance of salt-responsive genes and transcription factors (Flowers and Colmer, 2008; Rajalakshmi and Parida, 2012; Himabindu *et al.*, 2016). In more recent studies, the therapeutic uses have been validated by in silico analysis. This showed that the three selected isoflavones had high ADME properties and very low

toxicity, as measured by a number of online toxicity analysis tools.

So, the metabolic shifting of isoflavones after priming with chitosan and nano-chitosan may help mung bean seedlings handle salt stress better, and mitigate the adverse effect of oxidative stress (Sen *et al.*, 2020; Zayed *et al.*, 2017).

### Conclusion

The current study reveals that SMP with nano-chitosan may increase the Genistein content in mung bean sprouts showing the metabolic shifting of important isoflavones with potential therapeutic applications, while also producing functional foods enriched with nutritional value and health advantages. Thus, mung bean sprouts are a well-known healthier alternative, and because of their potential effects on human health and the industry's rapid expansion, nutritional fortification of this food has become an important topic of study.

### LIST OF FIGURES

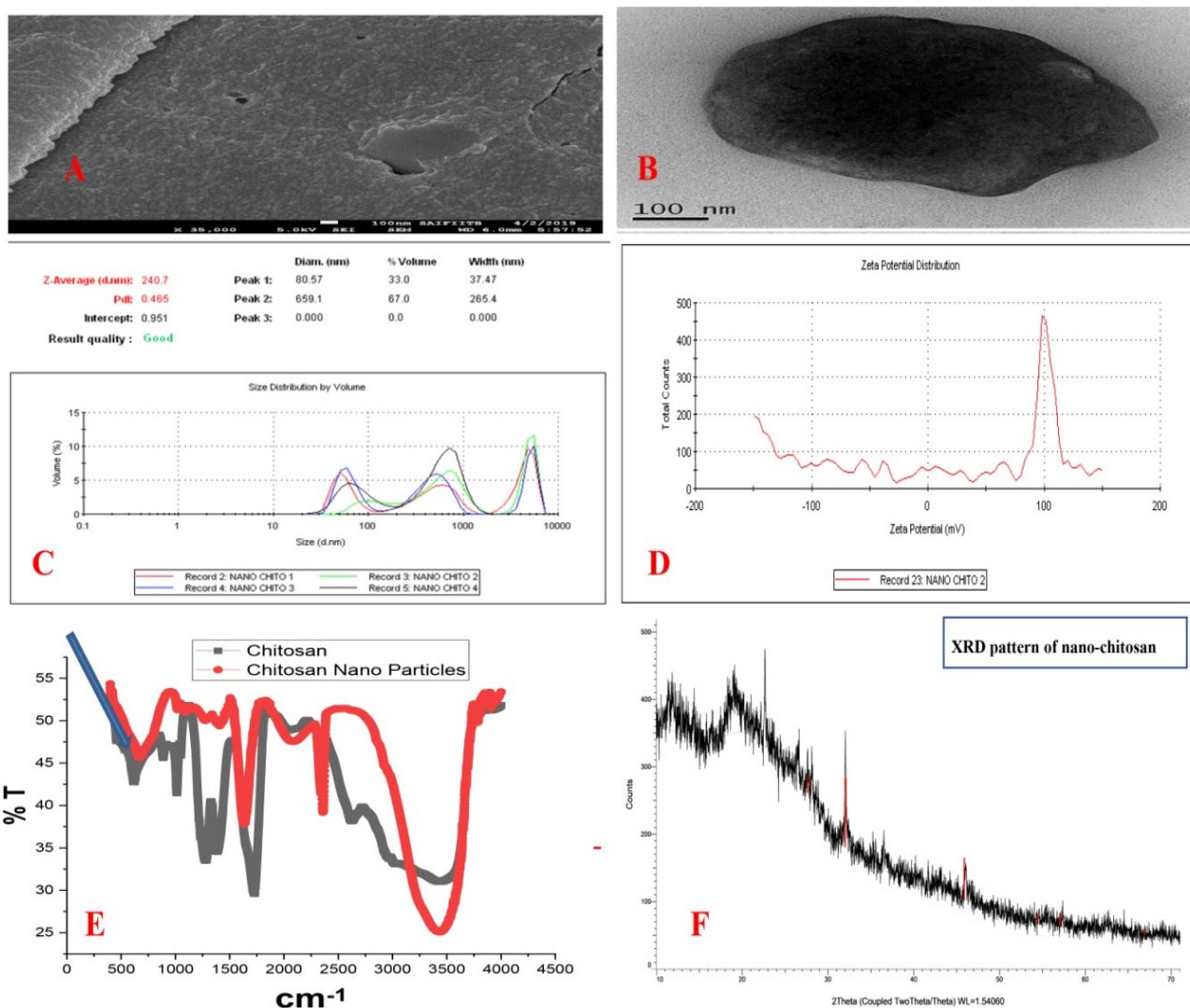


**Fig. 1 (A-F):** Characterization of nano-chitosan, (A) SEM of nano-chitosan, (B) TEM of nano-chitosan, (C) DLS of nano-chitosan, (D) Zeta potential of nano-chitosan, (E) FTIR spectra of chitosan & nano-chitosan, (F) XRD spectra of nano-chitosan

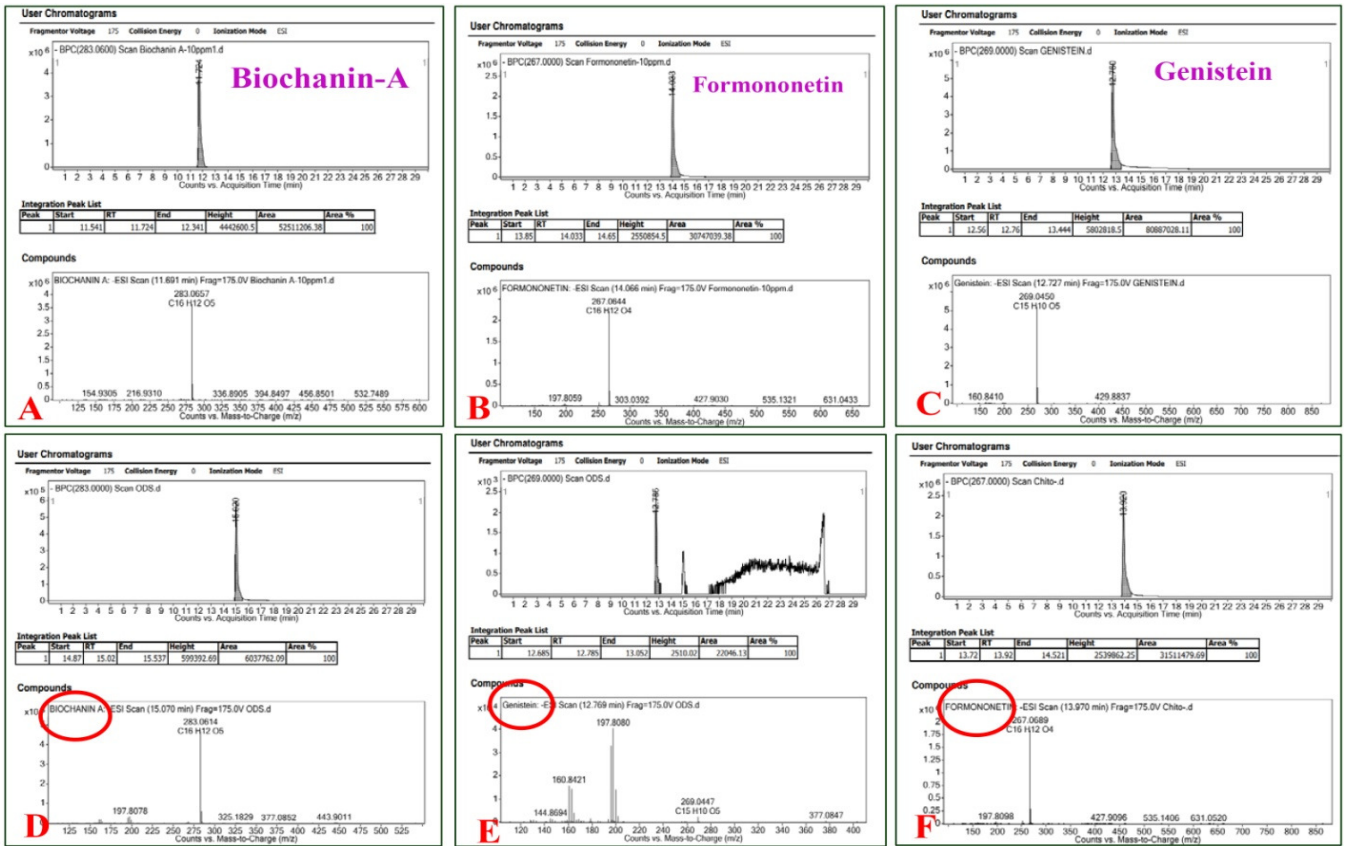


**Fig. 2:** Quantitative LC-MS analysis of three standard isoflavones (A, B, and C) and major identified isoflavones in untreated control, nano chitosan primed and chitosan primed mung bean seedlings respectively (D, E, and F)

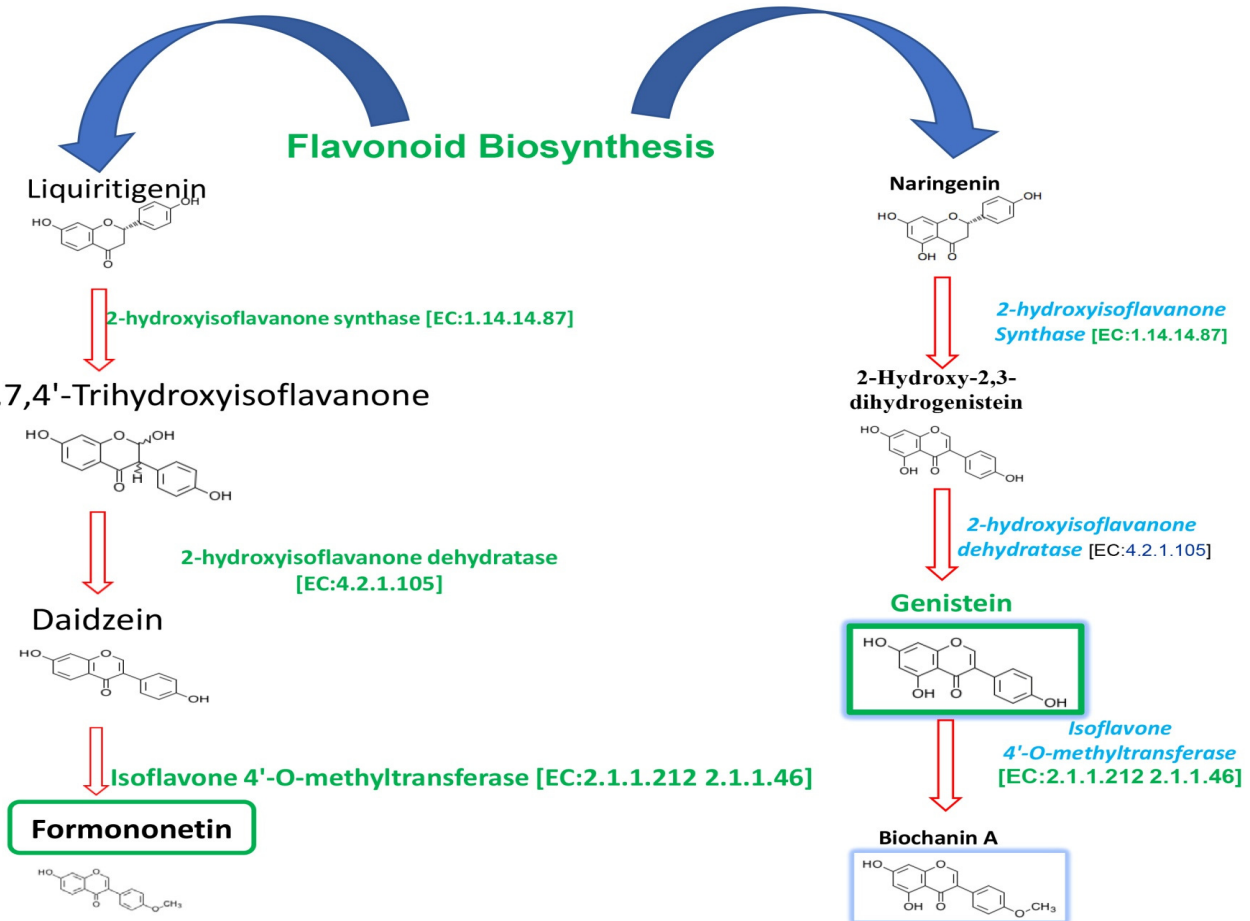


**Fig. 3:** Derivation and glycosylation of Biochanin-A, Genistein and Formononetin through the KEGG pathway

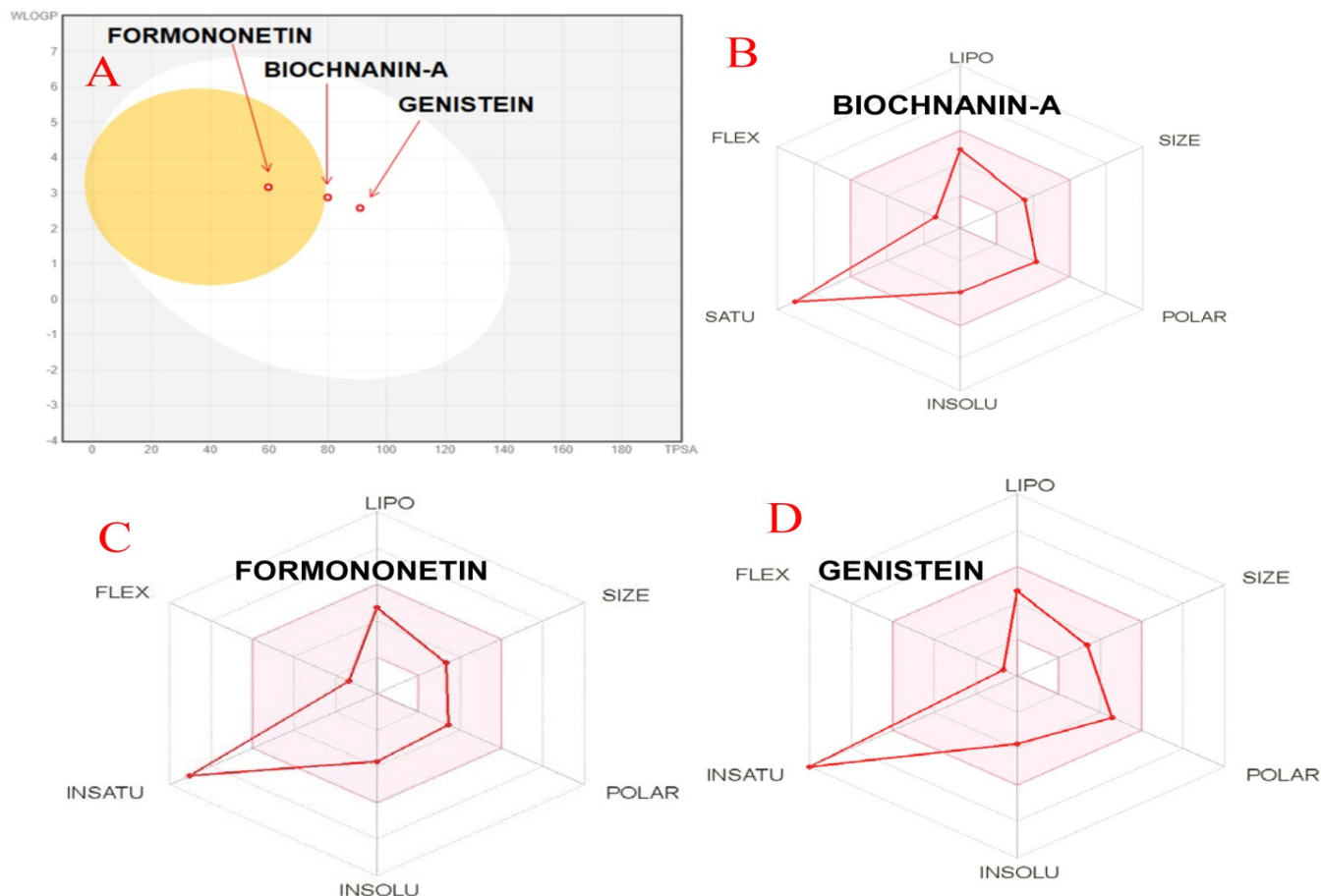


**Fig. 4 (A-D):** BOILED-Egg predictive model (A) and Radar diagrams (B-D) for Biochanin A, Formononetin, and Genistein

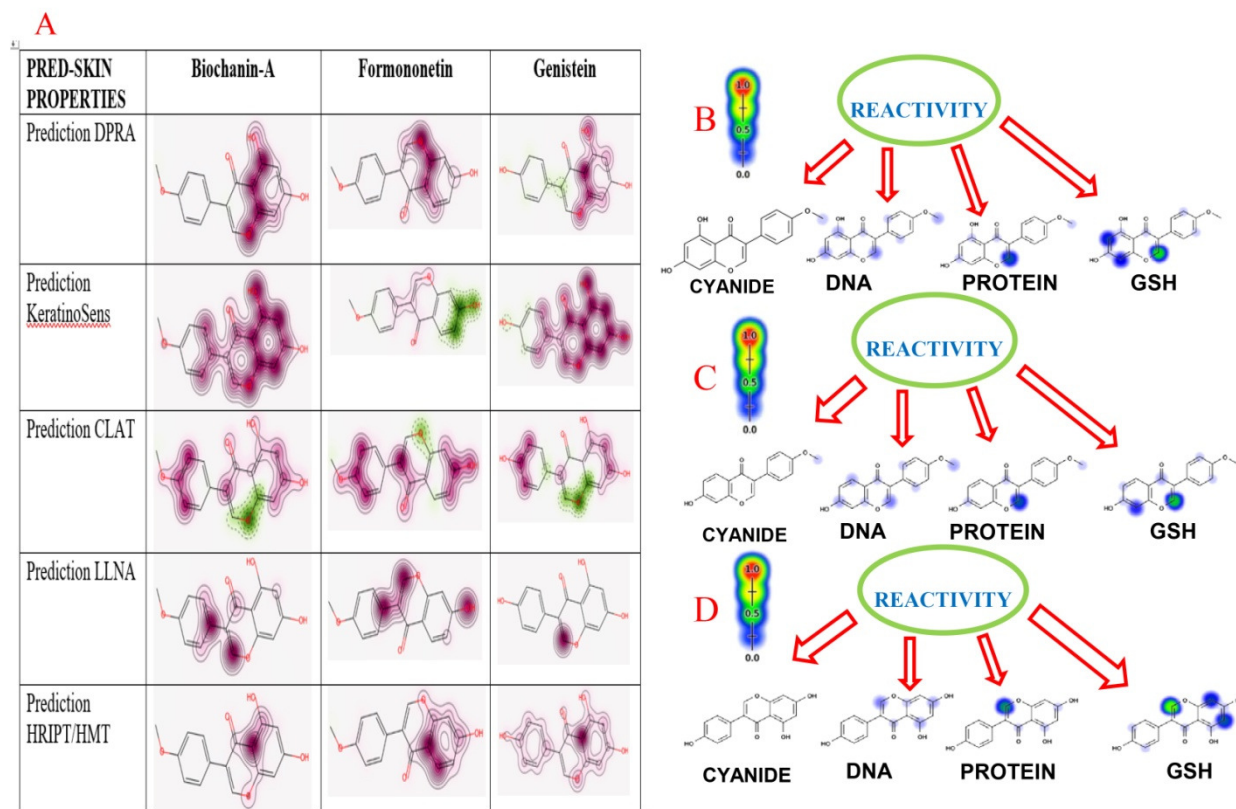


**Fig. 5 (A-D):** PRED SKIN properties (A) with their respective probability maps and DNA reactivity diagrams (B-D) of the possible metabolites of phase I metabolism of Biochanin A, Formononetin and Genistein respectively predicted using xenosite reactivity

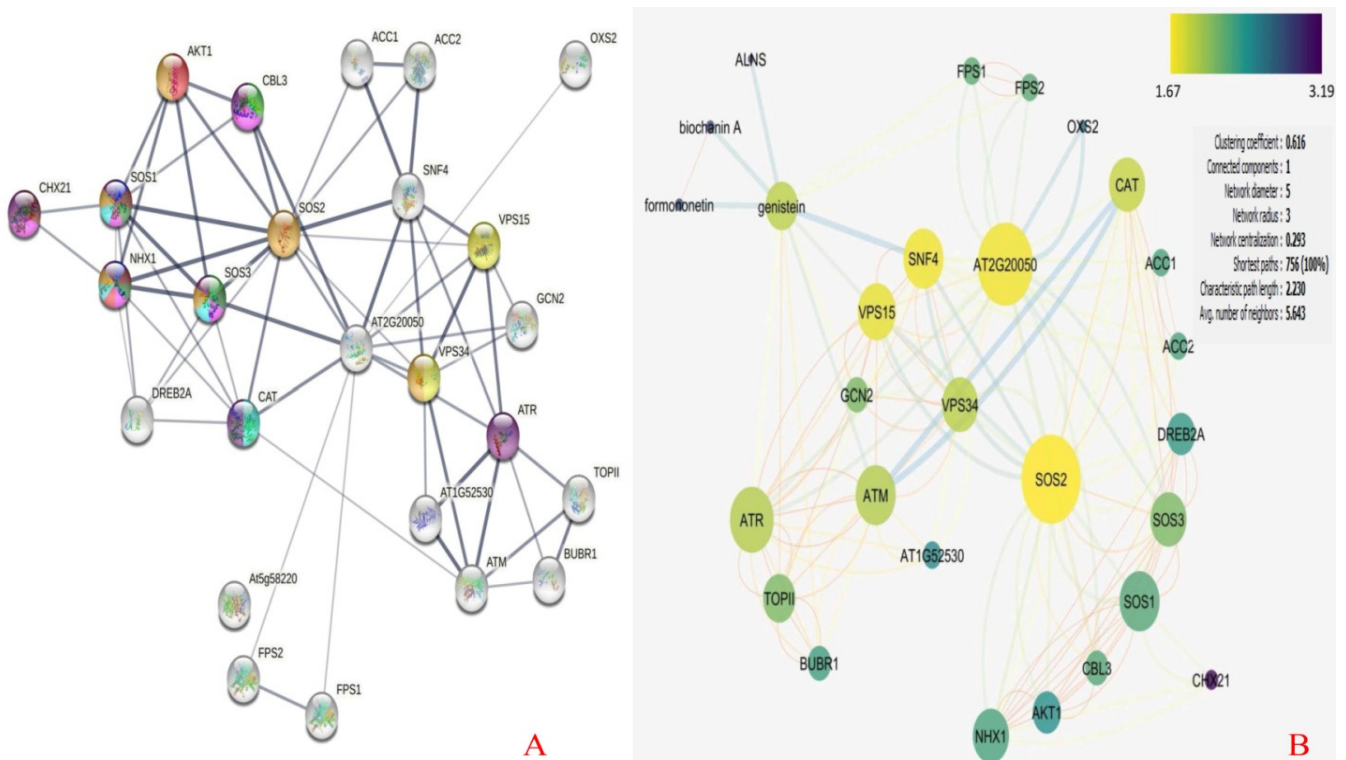


**Fig. 6 (A-B):** STRING (A) and Cytoscape analysis (B) to ascertain how the isoflavones interact with the salt stress genes. The response to salt stress involves SOS1, SOS2, SOS3, CBL3, NHX1, AKT1, and VPS34.

#### Author contributions

Concept, Design, & Supervision (PM & JB), Materials (SKS), Data Collection and/or Processing (SKS), Analysis and/or Interpretation (JB), Literature Search (SKS), Writing (SKS), Critical Reviews (JB & SKS). SKS= Sujoy Kumar Sen, PM= Palash Mandal, JB= Jnan Bikash Bhandari

#### Acknowledgments

The authors would like to express their gratitude to Mr. Kushankur Sarkar for his assistance with the Cytoscape study.

#### Conflicts of interest

There are no apparent conflicts of interest.

#### References

- Basketter, D.A.; Evans, P.; Fielder, R.J.; Gerberick, G.F.; Dearman, R.J. and Kimber, I. (2002). Local lymph node assay—validation, conduct and use in practice. *Food and Chemical Toxicology*, 40(5): 593-598.
- Bezek, Š.; Ujházy, E.; Mach, M.; Navarová, J.; and Dubovický, M. (2008) Developmental origin of chronic diseases: toxicological implication. *Interdisciplinary toxicology*, 1(1): 29-31.
- Birt, D.F.; Hendrich, S. and Wang, W. (2001) Dietary agents in cancer prevention: flavonoids and isoflavonoids. *Pharmacology and therapeutics*, 90(2-3): 157-177.
- Cao, D.; Li, H.; Yi, J.; Zhang, J.; Che, H.; Cao, J.; Yang, L.; Zhu, C. and Jiang, W. (2011). Antioxidant properties of the mung bean flavonoids on alleviating heat stress. *PLoS one*, 6(6): e21071.
- Chen, Q.; Zhang, M. and Shen, S. (2011). Effect of salt on malondialdehyde and antioxidant enzymes in seedling roots of Jerusalem artichoke (*Helianthus tuberosus* L.). *Acta Physiologiae Plantarum*, 33: 273-278.
- Daina, A.; Michielin, O. and Zoete, V. (2017). Swiss ADME: a free web tool to evaluate pharmacokinetics, drug-likeness and medicinal chemistry friendliness of small molecules. *Scientific Reports*, 7(1): 42717.
- Delannée, V.; Langouët, S.; Siegel, A. and Théret, N. (2019). In silico prediction of Heterocyclic Aromatic Amines metabolism susceptible to form DNA adducts in humans. *Toxicology Letters*, 300: 18-30.
- Di, L.; Artursson, P.; Avdeef, A.; Ecker, G.F.; Faller, B.; Fischer, H.; Houston, J.B.; Kansy, M.; Kerns, E.H.; Krämer, S.D.; Lennernäs, H. and Sugano, K. (2012). Evidence-based approach to assess passive diffusion and carrier-mediated drug transport. *Drug discovery today*, 17(15-16): 905-912. <https://doi.org/10.1016/j.drudis.2012.03.015>
- Djombou-Feunang, Y.; Fiamoncini, J.; Gil-de-la-Fuente, A.; Greiner, R.; Manach, C. and Wishart, D.S. (2019) BioTransformer: a comprehensive computational tool for small molecule metabolism prediction and metabolite identification. *Journal of cheminformatics*, 11(1): 1-25.
- Dubin, S.B.; Lunacek, J.H. and Benedek, G.B. (1967). Observation of the spectrum of light scattered by solutions of biological macromolecules. *Proceedings of the National Academy of Sciences*, 57(5): 1164-1171.
- Egan, W.J.; Merz, K.M. and Baldwin, J.J. (2000) Prediction of drug absorption using multivariate statistics. *Journal of medicinal chemistry*, 43(21): 3867-3877.
- Farooq, M.; Aman, U.; Lee, D. and Alghamdi, S.S. (2018). Terminal drought-priming improves the drought tolerance in desi and kabuli chickpea. *International Journal of Agriculture and Biology*, 20(5): 1129-1136. <https://doi.org/10.1111/j.1469-8137.2008.02531.x>
- Flowers, T.J. and Colmer, T.D. (2008). Salinity tolerance in halophytes. *New phytologist*, 945-963. <https://doi.org/10.1111/j.1469-8137.2008.02531.x>

- Ghose, A.K.; Viswanadhan, V.N. and Wendoloski, J.J. (1999). A knowledge-based approach in designing combinatorial or medicinal chemistry libraries for drug discovery. 1. A qualitative and quantitative characterization of known drug databases. *Journal of combinatorial chemistry*, 1(1): 55-68. <https://doi.org/10.1021/cc9800071>
- Himabindu, Y.; Chakradhar, T.; Reddy, M.C.; Kanygin, A.; Redding, K.E. and Chandrasekhar, T. (2016) Salt-tolerant genes from halophytes are potential key players of salt tolerance in glycophytes. *Environmental and Experimental Botany*, 124: 39-63. <https://doi.org/10.1016/j.envexpbot.2015.11.010>
- Janicka-Russak, M.; Kabała, K. and Burzyński, M. (2012) Different effect of cadmium and copper on H<sup>+</sup>-ATPase activity in plasma membrane vesicles from *Cucumis sativus* roots. *Journal of Experimental Biology*, 63: 4133–4142. <https://doi.org/10.1093/jxb/ers097>.
- Lamartiniere, C.A.; Murrill, W.B.; Manzollillo, P.A.; Zhang, J.X.; Barnes, S.; Zhang, X.; Wei, H. and Brown, N.M. (1998) Genistein alters the ontogeny of mammary gland development and protects against chemically-induced mammary cancer in rats. *Proceedings of the Society for Experimental Biology and Medicine*, 217(3): 358-364.
- Lipinski, C.A.; Lombardo, F.; Dominy, B.W. and Feeney, P.J. (2012). Experimental and computational approaches to estimate solubility and permeability in drug discovery and development settings. *Advanced drug delivery reviews*, 64: 4-17.
- Martz, F.; Sutinen, M.L.; Kiviniemi, S. and Palta, J.P. (2006). Changes in freezing tolerance, plasma membrane H<sup>+</sup>-ATPase activity and fatty acid composition in *Pinus resinosa* needles during cold acclimation and de-acclimation. *Tree physiology*, 26(6): 783-790. <https://doi.org/10.1093/treephys/26.6.783>.
- Mir, R.H.; Sabreen, S.; Mohi-ud-din, R.; Wani, T.U.; Jaleel, A.; Jan, R.; Banday, N.; Maqbool, M.; Mohi-ud-din, I.; Mir, B. I. and Ahmad, G. (2022) Isoflavones of Soy: Chemistry and Health Benefits. In *Edible Plants in Health and Diseases: Volume 1: Cultural, Practical and Economic Value* (pp. 303-324). Singapore: Springer Nature Singapore.
- Muegge, I.; Heald, S.L. and Brittelli, D. (2001). Simple selection criteria for drug-like chemical matter. *Journal of medicinal chemistry*, 44(12): 1841-1846.
- Raies, A.B. and Bajic, V.B. (2016). In silico toxicology: computational methods for the prediction of chemical toxicity. *Wiley Interdiscip Rev Comput Mol Sci*. 6(2): 147-172. <https://doi.org/10.1002/wcms.1240>
- Rajalakshmi, S.; and Parida, A. (2012) Halophytes as a source of genes for abiotic stress tolerance. *Journal of Plant Biochemistry and Biotechnology*, 21: 63-67. <https://doi.org/10.1007/s13562-012-0146-x>
- Rajeshwari, K.; Latha, S.; Gomathi, T.; Sangeetha, K.; and Sudha, P.N. (2016) Preparation and Characterisation study of Nanochitosan (NCS) and polyvinyl alcohol (PVA) binary blends with glutaraldehyde as a crosslinking agent. *Der Pharmacia Lettre*, 8(19): 485-495.
- Reiter, R.; Paredes, S.; Korkmaz, A.; Jou, M.J. and Tan, D.X. (2008) Melatonin combats molecular terrorism at the mitochondrial level. *Interdisciplinary Toxicology*, 1(2): 137-149.
- Ryan-Borchers, T.A.; Park, J.S.; Chew, B.P.; McGuire, M.K.; Fournier, L.R. and Beerman, K.A. (2006) Soy isoflavones modulate immune function in healthy postmenopausal women. *The American journal of clinical nutrition*, 83(5): 1118-1125.
- Sen, S.K.; Chouhan, D.; Das, D.; Ghosh, R. and Mandal, P. (2020) Improvisation of salinity stress response in mung bean through solid matrix priming with normal and nano-sized chitosan. *International journal of biological macromolecules*, 145: 108-123. <https://doi.org/10.1016/j.ijbiomac.2019.12.170>
- Shi, P. and Gu, M. (2020). Transcriptome analysis and differential gene expression profiling of two contrasting quinoa genotypes in response to salt stress. *BMC Plant Biology*, 20(1): 1-5.
- Sivakami, M.S.; Gomathi, T.; Venkatesan, J.; Jeong, H.S.; Kim, S.K. and Sudha, P.N. (2013) Preparation and characterization of nano chitosan for treatment wastewaters. *International journal of biological macromolecules*, 57: 204-212.
- Veber, D.F.; Johnson, S.R.; Cheng, H.Y.; Smith, B.R.; Ward, K.W. and Kopple, K.D. (2002). Molecular properties that influence the oral bioavailability of drug candidates. *Journal of medicinal chemistry*, 45(12): 2615-2623.
- Wang, H. J.; and Murphy, P. A. (1994) Isoflavone content in commercial soybean foods. *Journal of agricultural and food chemistry*, 42(8): 1666-1673. <https://doi.org/10.1021/jf00044a016>
- Wang, J. and Skolnik, S. (2009). Recent advances in physicochemical and ADMET profiling in drug discovery. *Chemistry and biodiversity*, 6(11): 1887-1899.
- Wang, L.; Wang, C.; Liu, X.; Cheng, J.; Li, S.; Zhu, J.K. and Gong, Z. (2019) Peroxisomal  $\beta$ -oxidation regulates histone acetylation and DNA methylation in Arabidopsis. *Proceedings of the National Academy of Sciences*, 116(21): 10576-10585. <https://doi.org/10.1073/pnas.1904143116>
- Yamagata, K. and Yamori, Y. (2021) Potential effects of soy isoflavones on the prevention of metabolic syndrome. *Molecules*, 26(19): 5863.
- Yu, P.; Kirkpatrick, R.J.; Poe, B.; McMillan, P.F. and Cong, X. (1999) Structure of calcium silicate hydrate (C-S-H): Near-, Mid-, and Far- infrared spectroscopy. *Journal of the American Ceramic Society*, 82(3): 742-748.
- Yuan, F.; Lyu, M.J.A.; Leng, B.Y.; Zhu, X.G. and Wang, B.S. (2016). The transcriptome of NaCl-treated *Limonium bicolor* leaves reveals the genes controlling salt secretion of salt gland. *Plant molecular biology*, 91: 241-256. <https://doi.org/10.1007/s11103-016-0460-0>
- Zayed, M.M.; Elkafafi, S.H.; Zedan, A.M. and Dawoud, S.F. (2017). Effect of nano chitosan on growth, physiological and biochemical parameters of *Phaseolus vulgaris* under salt stress. *Journal of Plant Production*, 8(5): 577-585.
- Zhang, L.; Ai, H.; Chen, W.; Yin, Z.; Hu, H.; Zhu, J.; Zhao, J.; Zhao, Q.; and Liu, H. (2017). CarcinoPred-EL: Novel models for predicting the carcinogenicity of chemicals using molecular fingerprints and ensemble learning methods. *Scientific reports*, 7(1): 2118.